Materials Research Bulletin 63 (2015) 6–12

Contents lists available at ScienceDirect

Materials Research Bulletin

journal homepage: www.elsevier.com/locate/matresbu

Structural, magnetic, and electrochemical properties of $LiMn_{1-x}Ni_xPO_4$

A. Ottmann [a,*], C. Jähne [a], H.-P. Meyer [b], R. Klingeler [a,c]

[a] Kirchhoff Institute for Physics, Heidelberg University, 69120 Heidelberg, Germany
[b] Institute of Earth Sciences, Heidelberg University, 69120 Heidelberg, Germany
[c] Centre for Advanced Materials, Heidelberg University, 69120 Heidelberg, Germany

ARTICLE INFO

Article history:
Received 23 June 2014
Received in revised form 31 October 2014
Accepted 2 November 2014
Available online 6 November 2014

Keywords:
B. Solvothermal
C. X-ray diffraction
D. Electrochemical properties
D. Magnetic properties

ABSTRACT

A solid solutions series of $LiMn_{1-x}Ni_xPO_4$ nanomaterials with $0 \leq x \leq 0.45$ was produced by a low-temperature microwave-assisted hydrothermal process. The materials have been systematically studied regarding structure, morphology, magnetism, and electrochemical properties. The lattice parameters in the orthorhombic olivine structure obey Vegard's law and linearly depend on x. Similarly, the static magnetisation reflects the decrease of the transition metal paramagnetic moment upon substitution of Mn^{2+} by Ni^{2+}. At low temperatures, antiferromagnetic long range order appears for all Ni-concentrations. The potential of the $Mn^{2+/3+}$ redox couple is found to linearly increase with x. This is explained by a larger electronegativity of Ni^{2+} as compared to Mn^{2+} and associated changes in the covalency of the Mn–O bond.

© 2014 Elsevier Ltd. All rights reserved.

1. Introduction

Since the introduction of $LiFePO_4$ as cathode material for lithium-ion batteries by Padhi et al. in 1997 [1], plenty of research has been dedicated to the olivine-structured orthophosphates. Major efforts focus on enhancing the poor electronic conductivity and ionic diffusivity in these materials [2,3], which is essential for application in lithium-ion batteries. In the case of $LiFePO_4$, these efforts resulted in a low cost, environmentally benign, and thermally stable material, which is applied commercially [4,5]. Due to the demand for higher energy densities, the phospho-olivines $LiMPO_4$ with M = Mn, Co, Ni are gaining increasing attention, as the redox couples exhibit a considerably higher potential vs. lithium, namely 4.1 V ($Mn^{2+/3+}$), 4.8 V ($Co^{2+/3+}$) and 5.2 V ($Ni^{2+/3+}$) [6–8]. $LiMnPO_4$ is of particular interest because the operating voltage does not exceed the electrochemical stability window of conventional electrolytes [9] and manganese is abundant as well as nontoxic. However, $LiMnPO_4$ features poor electrochemical properties due to an even lower electronic conductivity compared to $LiFePO_4$ and a Jahn–Teller distortion associated with Mn^{3+} in the delithiated phase [10–12]. Nanoscaling and Mn-site doping are promising approaches to overcome these drawbacks [13]. To be specific, Mn-site doping with smaller ions, e.g. Ni^{2+}, has been found to attenuate the lattice distortion, thereby improving the electrochemical performance [14,15]. Furthermore, mixed transition metal ion orthophosphates $LiM_{1-x}M'_xPO_4$ (M, M′ = Fe, Mn, Co) show an increase of the cell voltage [16], which presents an additional way to boost the energy density of cathode materials.

While conventional hydrothermal methods have been well established for decades, the more recent microwave-assisted approach combines the low-temperature synthesis with particularly short reaction times [17]. Moreover, it allows to tailor the size, morphology, and chemical composition of the product materials [18,19]. In case of the phospho-olivines, the hydrothermal route has been successfully applied to synthesise a broad range of doped and mixed transition metal compounds [17,20–23]. In the present work, a modified glycol-based synthesis protocol from Ref. [22] was adapted to obtain a $LiMn_{1-x}Ni_xPO_4$ doping series in 5%-steps up to $x = 0.45$. The data show solid solution behaviour with decreasing unit cell volume towards $LiMn_{0.55}Ni_{0.45}PO_4$, corresponding to Vegard's law and a rising reduction potential of the $Mn^{2+/3+}$ couple.

2. Experimental

$LiMn_{1-x}Ni_xPO_4$ powder samples were synthesised via a microwave-assisted hydrothermal route (cf. Ref. [24]). At first, manganese(II) and nickel(II) acetate tetrahydrate (Sigma–Aldrich) were dissolved in ethylene glycol (EG, Sigma–Aldrich) in a molar ratio of $(1-x):x$ with a total concentration of 0.03 mol l^{-1}. 10 ml of this solution was poured in a 30 ml glass vessel and aqueous solutions of lithium hydroxide (Sigma–Aldrich) and phosphoric

* Corresponding author. Tel.: +49 6221549819; fax: +49 6221549869.
E-mail address: alex.ottmann@kip.uni-heidelberg.de (A. Ottmann).

http://dx.doi.org/10.1016/j.materresbull.2014.11.008
0025-5408/© 2014 Elsevier Ltd. All rights reserved.

acid (85%, Merck) with concentrations of 1.5 mol l^{-1} and 1.0 mol l^{-1}, respectively, were added to obtain a (Mn+Ni):Li:P molar ratio of 1:1:1. The resulting mixture was heated in a *Monowave 300* (Anton Paar) microwave reactor within 10 min to 300 °C and kept at this temperature for 15 min while being stirred at 300 rpm. Natural cooling to room temperature was supported by compressed air flow inside the reactor. The resulting precipitate was recovered and washed five times by adding 12 ml of ethanol, centrifugating the suspension at 5000 rpm for 5 min and removing supernatant solution to ensure that no ethylene glycol and soluble precursors were left. Yields from three consecutive syntheses with the same precursor solution were dispersed together in ethanol in order to obtain the final product. Finally, this mixture was dried at ca. 100 °C overnight.

X-ray powder diffraction (XRD) was carried out on a Siemens *D500* in Bragg-Brentano geometry, applying Cu-$K_{\alpha 1}$ radiation and 2θ angle steps of 0.01°. Rietveld refinement with a pseudo-Voigt-type profile was done with the FullProf program [25]. This analysis was based on structure parameters for $LiMnPO_4$ (ICSD #99858 [26]). The morphology was studied by means of scanning electron microscopy (SEM) on a Zeiss *LEO 1530*. Elemental analyses were done by means of energy-dispersive X-ray spectrometry (EDX) on a *LEO 440*. Preliminarily, the samples were coated with gold (morphology studies) or carbon (elemental analyses), respectively. The calibration of the EDX-detector was checked by measuring the well-known end member $LiMnPO_4$. Magnetic properties have been determined with a Quantum Design *MPMS-2* after cooling in zero magnetic field (zfc).

Electrochemical characterisation by means of cyclic voltammetry was performed in two-electrode Swagelok-type cells vs. lithium metal with a *VMP3* multichannel potentiostat (Bio-Logic). The working electrodes were prepared from a mixture of pristine $LiMn_{1-x}Ni_xPO_4$ powders with carbon black (Timcal) and polyvinylidene fluoride (PVDF) binder (Solvay Plastics) in a weight ratio of 75:20:5. This mixture was pestled in a mortar under dropwise addition of N-methyl-2-pyrrolidone (NMP, Sigma–Aldrich). Around 4 mg of the resulting slurry was pasted on alumina meshes with a diameter of 10 mm, dried in vacuum at 100 °C overnight, pressed with 10 MPa and dried at 100 °C again. The cells were assembled in an Ar-atmosphere glove box (O_2/H_2O <1 ppm), where the working electrode and a lithium metal foil disk (Alfa Aesar), which had been pressed on a nickel current collector, were merged. Both electrodes were separated by two layers of glass microfibre (Whatman *GF/D*), soaked with 200 µl electrolyte. A 1 molar solution of $LiPF_6$ in 1:1 ethylene carbonate (EC)/dimethyl carbonate (DMC) was used as an electrolyte (Merck Electrolyte *LP30*). The active material mass per mesh area averaged 3.8 mg cm^{-2}. Electrochemical cycling was performed in the potential range 3.5–4.5 V at a scan rate of 0.05 mV s^{-1}, and in a climate chamber that was at 25 °C.

3. Results and discussion

The synthesis yields polycrystalline powders whose colour and morphology depend on the ratio between manganese and nickel in the precursor solution. Upon increasing the Ni content, the colour changes from cream white to light orange. Concomitantly, needle-like structures observed for $x = 0$ change to rhomb-like platelets, as displayed in the SEM images shown in Fig. 1. Since all synthesis parameters except the Mn:Ni ratio are kept constant, one has to conclude that differences between the transition metal ions are governing the morphology changes. Following Refs. [27,19] suggest that differences in acidity and electronegativity are key factors. To be specific, Mn^{2+} (Ni^{2+}) shows $pK_a = 10.59$ (9.86) and EN = 1.55 (1.91) [28]. One may hence speculate that in case of Ni^{2+}, the crystallite surfaces are decorated more efficiently by OH^- and EG–O^- which affects the crystal growth accordingly.

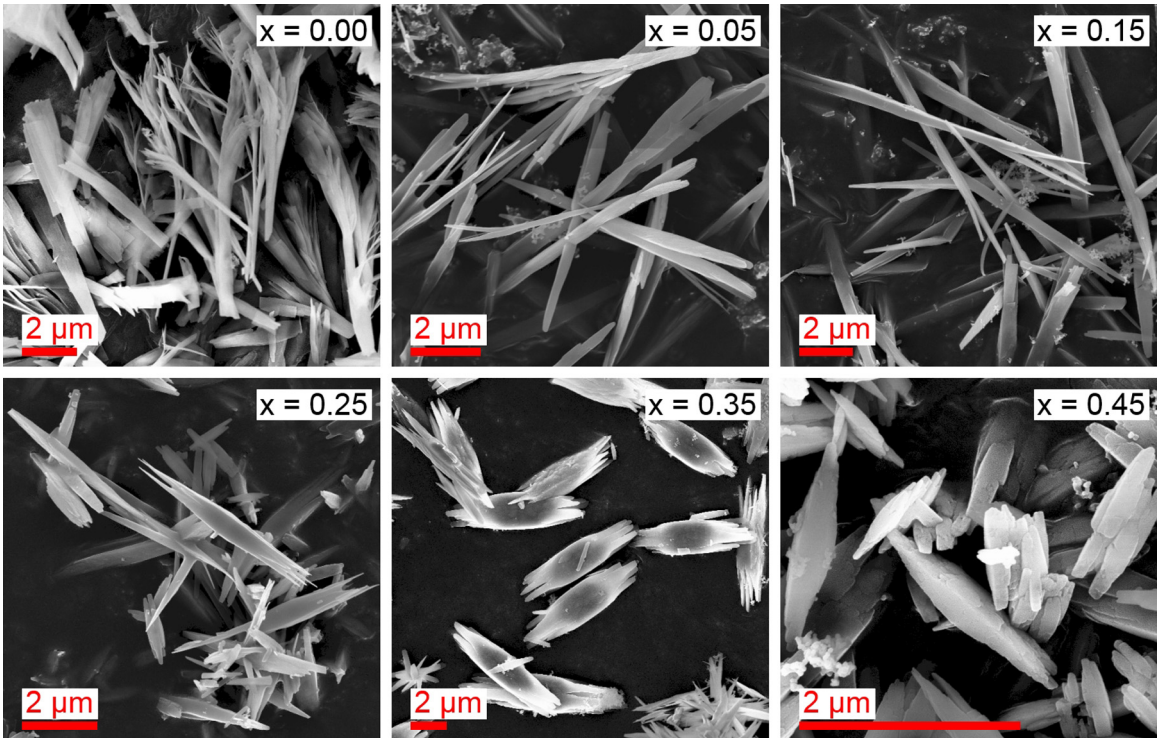

Fig. 1. SEM images of pristine $LiMn_{1-x}Ni_xPO_4$ with $0 \leq x \leq 0.45$.

Download English Version:

https://daneshyari.com/en/article/7905585

Download Persian Version:

https://daneshyari.com/article/7905585

Daneshyari.com